DOI: https://doi.org/10.14256/JCE.3036.2020
Građevinar 1/2021

Primljen / Received: 13.8.2020.
Ispravljen / Corrected: 15.10.2020.
Prihvaćen / Accepted: 16.11.2020.
Dostupno online / Available online: 10.2.2021.

Fragility and robustness analysis of a multistorey RC building

Authors:

Miloš Čokić, MSc. CE
University of Novi Sad, Serbia
Faculty of Technical Sciences
cokicmilos@gmail.com
Corresponding author

Prof.emer. **Radomir Folić**, PhD. CE
University of Novi Sad, Serbia
Faculty of Technical Sciences
folic@uns.ac.rs

Research Paper

Miloš Čokić, Radomir Folić

Fragility and robustness analysis of a multistorey RC building

The robustness of a reinforced concrete (RC) five-storey building (frame system stiffened by walls) is analysed in the paper. A high ductility class structure is designed in accordance with structural Eurocodes. The response of the structure to eight different scenarios of the ground floor vertical element loss is analysed. Nonlinear Static Analysis (NSA) and Nonlinear Dynamic Analysis (NDA) methods are used for the robustness analysis. Fragility curves of the building are derived from statistical analysis of these results. The values obtained through NSA and NDA, damage limit states of the system, and fragility curves, are compared. The influence of the position of the removed element on robustness of the structure is also analysed.

Key words:
RC structure of a building, frame structure stiffened by walls, robustness, fragility, progressive collapse, nonlinear static analysis, nonlinear dynamic analysis, damage limit states

Znanstveni rad

Miloš Čokić, Radomir Folić

Analiza oštetljivosti i robusnosti višekatne armiranobetonske zgrade

U radu je analizirana robusnost armiranobetonske (AB) peteroetažne zgrade (okvir ukrućen zidovima). Konstrukcija visoke klase duktilnosti dimenzionirana je u skladu s nizom konstrukcijskih norma Eurokod. Analiziran je odziv konstrukcije za osam scenarija gubitka pojedinih vertikalnih elementa u prizemlju. Za analizu robusnosti primijenjene su metoda nelinearne statičke (NSA) i dinamičke analize (NDA). Statističkom obradom konstruirane su krivulje oštetljivosti zgrade. Uspoređene su vrijednosti dobivene primjenom NSA i NDA, granična stanja oštećenja sistema i krivulje oštetljivosti. Proučen je i utjecaj položaja uklonjenoga elementa na robusnost.

Ključne riječi:
AB konstrukcija zgrade, okvir ukrućen zidovima, robusnost, oštetljivost, progresivni slom, nelinearna statička analiza, nelinearna dinamička analiza, granična stanja oštećenja

Vorherige Mitteilung

Miloš Čokić, Radomir Folić

Schadens- und Robustheitsanalyse eines mehrstöckigen Stahlbetongebäudes

Die Arbeit analysiert die Robustheit eines fünfstöckigen Gebäudes aus Stahlbeton (SB) (durch Wände versteifter Rahmen). Eine Konstruktion mit hoher Duktilität wird in Übereinstimmung mit einer Reihe von Eurocode-Konstruktionsnormen dimensioniert. Die strukturelle Reaktion wurde in acht Szenarien des Verlusts einzelner vertikaler Elemente im Erdgeschoss analysiert. Für die Robustheitsanalyse wurden nichtlineare statische (NSA) und dynamische Analysemethoden (NDA) verwendet. Statistische Schadenskurven des Gebäudes wurden durch statistische Verarbeitung erstellt. Die mit NSA und NDA erhaltenen Werte, die Grenzzustände des Systemschadens und die Schadenskurve wurden verglichen. Der Einfluss der Position des entfernten Elements auf die Robustheit wurde ebenfalls untersucht.

Schlüsselwörter:
Stahlbeton-Baukonstruktion, durch Wände versteifter Rahmen, Robustheit, Beschädigung, fortschreitender Einsturz, nichtlineare statische Analyse, nichtlineare dynamische Analyse, Grenzzustände

1. Introduction and literature overview

Until the end of the 1960's, the traditional analysis of structures omitted action-loads called accidental or extraordinary loads; in the USA, they are called abnormal loads. They occur very rarely but often have significant consequences, i.e. progressive collapse of the structure. Depending on their intensity, sudden effects cause cracks and various damage to RC structures. Accidental actions, however, cause great damage, and even collapse. Therefore, it is necessary to assess the extent and location of damage and their effect on the integrity of the structure or the loss of bearing capacity of the system. After analysis of behaviour of buildings subjected to accidental actions, which lead to local or complete collapse, it was concluded that the worst damage is "suffered" by buildings designed without adequate continuity and joints of individual elements, and/or with elements of insufficient ductility. When local collapse of a structure occurs, a chain reaction takes place, i.e. the load is transferred to adjacent elements, which can lead to either partial or full collapse of a structure [1]. This phenomenon is called *progressive collapse* (PC). It is significantly larger in volume than local collapse, i.e. it is disproportionate to initial damage [2]. Progressive collapse of structures of multi-storey buildings usually occurs when one or more vertical supporting elements (columns or walls) suddenly lose their bearing capacity due to extreme actions imposed on the structure (terrorist attacks, vehicle impacts, gas explosions, etc.). The most comprehensive overview of numerical and experimental studies and technical regulations on progressive collapse, with comparative analysis, is presented in [1].

The collapse of a part of the Roman Point Tower in London on 16 May 1968 raised the level of interest in the study of progressive collapse. This was the reason for the introduction of this concept and the adoption of first technical regulations in Great Britain, in the early 1970s, and then in Canada [3] and the USA [4]. By 2010, the progressive collapse of several tall buildings led to major changes in regulations for the design of structures and their protection, as noted in [1]. Several extreme events and progressive collapse of structures, along with the dates of publication of relevant regulations and provisions, which followed these occurrences, are summarized in [3]. Since the beginning of the 21st century, there has been a growing interest in risk assessment associated with extreme effects, although they rarely occur [1], especially after the collapse of the World Trade Centre (WTC) Towers on 11 September 2011. The paper [5] is dedicated to acceptable risk in this field. In the European standards for the design of structures, the provisions on progressive collapse [6] were first introduced in 2002.

The concept of assessment of susceptibility of structures to progressive collapse and related definitions differ to some extent in various documents and papers published by individual authors. The structures of prefabricated concrete buildings are significantly more susceptible to progressive collapse than monolithic structures [7]. Studies relating to the behaviour of structures under earthquake action use a methodology that introduces the notion of fragility of buildings [8]. Fragility is a measure of loss [9]. Fragility curves provide insight into the probability of an event and the degree of damage or complete collapse of analysed structures. They can be used to assess the degree of damage to both existing and new buildings [10]. In this way, it is possible to gain insight into the threat to the usability of structures subjected to an earthquake or accidental action. The paper [8] discusses fragility of reinforced concrete structures that are used in Europe, while the study of parameters affecting PC is presented in [13]. Terms and definitions used in the analysis of progressive collapse and robustness, and ways to achieve robustness (insensitivity to local collapse), integrity, and ductility of reinforced concrete structures, are discussed in [7, 12].

In [12], a definition of robustness was proposed with risk assessment related to the level of robustness of the structure. *Robustness* represents the ability of a structural system to resist progressive collapse (PC) [12]. In [13], robustness is defined as follows: "the ability of a structure to withstand events such as fires, explosions, impacts, or the consequences of human error without the occurrence of damage that is disproportionate to the cause". In [1, 14], in addition to the above, several more definitions are presented in technical regulations [15-17] and the corresponding literature. A more complete consideration of robustness and its practical application is contained in [18, 19], and in dissertation [20]. Measures for achieving robustness, and robustness assessment, are discussed in detail in [21, 22]. Nonlinear analyses and parametric studies based on their application are used for a more accurate assessment of robustness [23].

The design of reinforced concrete buildings in accordance with requirements for the prevention of PC is discussed in [11], while the design of robustness based on risk optimization with uncertainty assessment is considered in [24]. Strategies for PC risk mitigation are discussed in [25]. Influential parameters for RC structures with regard to PC are considered in [26]. The problem of bearing capacity of hinges and sub-units as related to PC is discussed in [27, 28]. Energy-based methods of theoretical and experimental studies of PC are considered in [29, 30], while practical application of energy-based methods and the potential of PC are presented in [31]. According to papers [13, 32, 33], one or more of the following approaches can be applied in order to achieve adequate system robustness:

- structural measures: the extent of damage to structural system is limited; or the most important / key structural elements are designed to withstand any possible load,
- non-structural measures: reducing the likelihood of collapse-causing effects or reducing the intensity of the action (prevention); mitigation of the consequences of failure of system elements.

Most papers dealing with robustness and progressive collapse are concerned with RC frame structures [34, 42]. Much fewer papers analyse frame structures stiffened by walls – dual type, i.e. frame structures stiffened by RC walls. Paper [43] focuses on this type of structures and analyses the mechanism of resistance of such systems to progressive collapse. Paper [44] discusses mitigation of PC by activating the elastoplastic chain. The progressive collapse of multi-storey buildings depends on several parameters, namely on the type of structural system and its regularity, while the typology of collapse or collapse itself is described in detail in [45]. The FEM based analysis of PC of RC structures suffering column loss is discussed in [46]. Problems of progressive collapse of reinforced concrete structures exposed to earthquakes are discussed in [47, 48]. Paper [2] explains the phenomena of progressive collapse and proposes the above mentioned term *disproportionate collapse* for such collapse. Three alternative approaches to the design of structures resistant to disproportionate collapse are listed: improved interconnection of elements or establishment of the continuity of joints, removal of hazards and weak elements, and design of key elements. A summary of the state-of-the-art of methods used for assessing bearing capacity of building structures is presented in [49].

Progressive collapse is a dynamic process in which the system is constantly "searching" for alternative paths for the load. The loss of column is accompanied by large deflections, and the load of the upper floors is transferred to adjacent beams and plates. Thus, the analysis of structural behaviour requires application of nonlinear methods, or energy-based methods [29, 30]. The evaluation of modelling procedures and column removal times for PC building structures is considered in [50]. The collapse does not occur immediately. Mechanisms contributing to the resistance to progressive collapse are: 1) The action of the sprocket of beams and beams with plates that allows load transfer to adjacent elements; 2). Wirendel action of rigid frames above the removed column; 3) Contribution of partitions and non-supporting elements (which is most often neglected). This is similarly described in [51]. The Applied Elements Method (AEM) is used in [36] to study progressive collapse due to seismic action for different column removal scenarios (angular, internal and external-facade). It was concluded that the performance of plate chain has the greatest effect on the resistance to PC. Even under the action of gravity load and earthquake, the angular column removal is the most critical part.

If robustness conditions are explicitly considered when designing a structural system, it should be checked whether the structure has a sufficient bearing capacity, and whether it can redistribute actions in the system through alternative paths [32, 52, 53]. Significant improvements in the definition and reliability of robustness enhancement methods are proposed in COST Action TU-06012 - Robustness of Structures [18] and in [54]. A review of the literature and regulations / standards (EN, USA, Canada, and UK), and recommendations for the design of monolithic and prefabricated reinforced concrete buildings, are presented in [7]. A broader literature review on progressive collapse resistance assessment, and other aspects of robustness and progressive collapse, is given in [55]. A more extensive overview of experimental research on PC in RC buildings is presented in [56]. This paper has contributed to the current more realistic knowledge on progressive collapse and robustness of buildings and their sub-units.

The possibility of preventing collapse of tall buildings, and methods of structural analysis, are discussed in the work of F. Fu [57]. Four methods for analysing behaviour of a structural system in the case of column removal are proposed in [20]: linear static, linear dynamic, nonlinear static, and nonlinear dynamic analysis. For assessing resistance to PC, the paper [58] describes and applies incremental dynamic analysis in vertical direction, while the methods for designing building structures with an increased resistance to PC are described in [58].

Apart from the indisputable importance in the design of new structures, the analysis of the existing buildings is also important, because they are the ones that suffer the greatest amount of damage, especially after seismic action. In this respect, the performance of damaged buildings is considered in [60] for several scenarios of vertical collapse, by also introducing the structural damage coefficient. The paper [61] presents the results of the analysis of structural systems of buildings that serve as basis for defining bearing capacity of new and existing buildings and their effect on PC. The criteria for existing buildings are presented in [62]. In the United States, documents [10, 63] are used for seismic assessment, rehabilitation, and reinforcement of structures. Assessment of nonlinear behaviour of concrete structures with PC-related damage is considered in [64, 65]. A similar procedure for the analysis of PC in RC buildings with wall-stiffened frame systems is presented in [66], while numerical simulations for studying PC in RC buildings are discussed in [67].

References [68, 71, 72] and methods described in [73] are used to calculate the structure. In addition, methods presented in [74, 80] are used in this paper. The influence of span length on PC of multi-storey buildings is considered in [81], while the influence of irregular structural system on progressive collapse is analysed in [82]. EN [83, 84] are used in the analysis of the structure with RC walls, while the procedure described in [85] is used for constitutive hinges of concrete and steel reinforcement. In addition to the above, the procedures described in [86] are also used in modelling the structure. A certain similarity can be observed between numerical procedures for the analysis of progressive collapse, and the analysis of structures exposed to earthquake action. The influence of the structure's ductility on progressive collapse of the system is investigated in [87], because [15] excludes ductility and residual bearing capacities, which is used in seismic design. The corresponding regulations can be used to reduce the likelihood of PC.

This paper analyses robustness of a five-storey RC building with frame structural system stiffened by RC walls, as well as its susceptibility to progressive collapse. The structure is designed as a high ductility class (DCH) system. in accordance with structural Eurocodes [6, 13, 83, 84]. Methods of nonlinear static analysis (NSA) and nonlinear dynamic analysis (NDA) are used to analyse robustness of the structure. The structural response in the scenarios involving the loss of a single vertical element on the ground floor of the building (column or wall) is analysed. Beam elements are modelled without and with the inclusion of the plate effective width, and the results are compared. The results of NSA and NDA are presented in the form of *pushdown* curves. *Pushdown* analyses are performed in accordance with the UFC [16, 17] and GSA [55] recommendations. The NDA is applied to determine damage limit states of the system. Using the methods of mathematical statistics and probabilities, the fragility curves of the AB building are made based on the methods used in mathematical statistics and probability assessment, and the probability of occurrence of damage limit states of the system are identified. The *pushdown* analysis results are compared, as well as the damage limit states of the system and the fragility curves. The influence of the removed element's position in the structural system, and its distance from the structure's centre of stiffness, on the element's ability to resist PC, is also analysed.

2. Materials and methods

2.1. Geometrical and physical characteristics of structural system

The subject of the analysis is a RC business-residential 5-storey building (ground floor + 4 floors). The structural system of the building is framed in the *X* direction, and the frame is stiffened by walls in the *Y* direction [84]. Main structural elements of the analysed building are reinforced concrete plates, beams, columns, and walls. The grid of the structural system is shown in Figure 1. The length of one span in both directions is 4.2 m (total 5 x 4.2 m), the height of the ground floor is 3.6 m, and the height of all other floors is 3.2 m, and so the building is 16.4 m in total height. In order to simplify the modelling process and calculation of the structure, all vertical elements are clamped at the bottom level of the structural system, i.e. the structure – ground interaction is not included in the calculation and design of the structure.

Properties of concrete C30 / 37 [83] and reinforcing steel class C (f_{yk} = 500 MPa, k = 1.15) [83] were adopted for the analysis of the model. The building is designed as a ductility class high (DCH) structural system [84]. The structure was designed in accordance with the methods and recommendations given in the European standards for building design [6, 13, 83, 84], while the calculations were performed using [71]. The structural system behaviour was analysed using nonlinear static analysis (NSA) and nonlinear dynamic analysis (NDA). Geometrical cross-section properties of structural elements are shown in Table 1. Parameters m_b and m_d in Table 1 represent cross section of the reinforcement for cross-section, where m_b is the cross section of the stirrups perpendicular to the width of the cross section *b*, and m_d is the cross section of the stirrups perpendicular to the length of the cross section *d*.

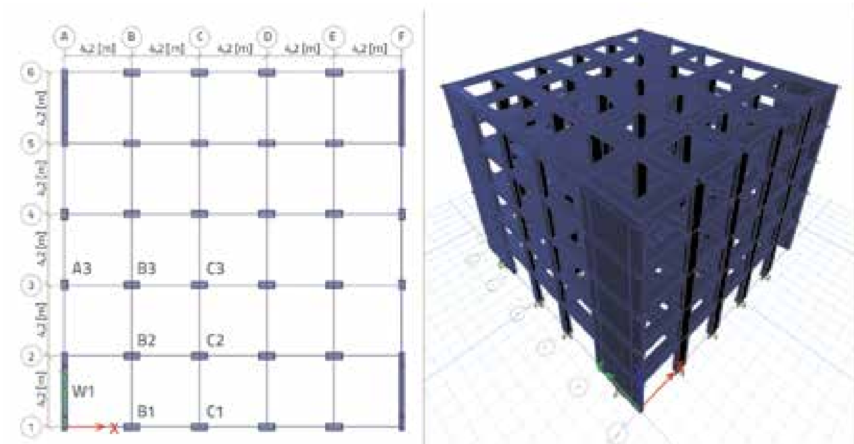

Figure 1. Base section and view of individual columns being removed for structure robustness analysis (left) and 3D model of the building (right)

Table 1. Geometric properties of structural elements

Element type	Dimension notation [cm]	Dimension [cm]	Reinforcement [longitudinal]-[traverse]
Plate effective width	$d_{pl}/b_{eff,i}$	55/14	Ø12/20
Beams in X direction	b_b/d_b	30/40	[3(upper zonea)+2(bottom zone) Ø20]-[Ø8/10] , $m_b = m_d = 2$
Facade beams in Y direction			[3+3 Ø18]-[Ø8/10] , $m_b = m_d = 2$
Internal beams in Y direction			[3+3 Ø14]-[Ø8/8] , $m_b = m_d = 2$
Facade beams in Y direction	b_c/d_c	40/60	[14 Ø16]-[Ø10/9] , $m_b = m_d = 4$
Svi ostali stupovi	b_c/d_c	40/100	[24 Ø20]-[Ø10/10] , $m_b = m_d = 4$
Rubni element zida	$b_{BE.}/l_{BE}$	30/80	[16 Ø22 (1. and 2. floor-critical zone)]-[Ø10/6] , $m_b = 2$, $m_d = 7$ [16 Ø16 (3., 4. i 5. floor)]-[Ø10/10] , $m_b = 2$, $m_d = 5$
Unutarnji element zida	$b_{IE.}/l_{IE}$	30/300	[50 Ø8]-[Ø16/20-horizontal (shear) reinforcement]

2.2. Robustness analysis scenarios

Bearing capacity loss scenarios were adopted for each individual column or wall on the ground floor in order to analyse robustness of the structural system. Since the structure is biaxially symmetrical at the base, it was sufficient to remove a quarter of structural elements on the ground floor for the analysis of the entire system, as shown in Figure 1 (left).

2.3. Loads and actions

The following loads act on the structure: dead load (*DL*) – the self weight of structural elements and additional constant load; live load (*LL*) and seismic load (S_j), which were used for the design of the structure. Gravity load combinations given in equations (1) and (2), and design values of parameters and methods for calculating robustness, were used for the nonlinear robustness analysis of the system, as given in documents [15, 16].

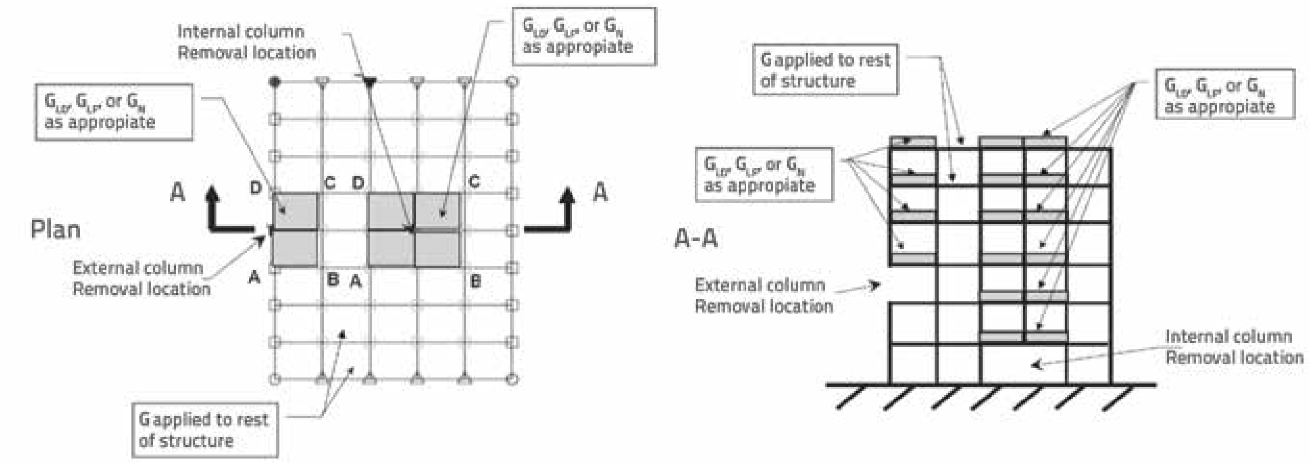

Figure 2. Application of NSA *pushdown* procedure in column removal, according to [16]

$$G = 1{,}2 \cdot DL + 0{,}5 \cdot LL \tag{1}$$

$$Q_R = G_{NSA} = G_{NDA} = \Omega \cdot (1{,}2 \cdot DL + 0{,}5 \cdot LL) = \Omega \cdot \mathrm{G} \tag{2}$$

where G is the combination of gravity loads, Q_R are increased gravity loads (IGL) acting on the structural system, and Ω is the dynamic increase factor (DIF) for the analysis of nonlinear behaviour of the system and structural robustness. In robustness analysis, DIF (Ω) increases incrementally until the point of collapse, desired state, or the point of non-convergence of the model, is reached. When applying both calculation methods (NSA and NDA), the structure is subjected to load in accordance with provisions given in [15, 16].

When the NSA *pushdown* method is applied, the first step is to apply gravity load (1) to the entire, previously unloaded structure model, according to the corresponding capacity loss scenarios for columns and the wall. After this step, the IGL combination (2) is applied only in the fields where the beams are in direct contact with the removed element (Figures 2 and 3), and the load (2) is applied on all floors above the removed element (Figures 2 and 3). The analysis of structural system continues by applying a combination of loads (2) and by gradually increasing the DIF (Ω) until the maximum reference-point displacement, or the state of collapse, is reached [15, 16].

When the NDA *pushdown* method is applied, the gravity load (1) is incrementally applied onto the entire unloaded system, in which the element predicted by the scenario has not as yet been removed, until the system equilibrium is reached. The replacement reactive load (RL) is applied for modelling the vertical element that will be removed. The RL represents reactions in the upper node of the removed element. Once the equilibrium is reached, the RL is removed according to an appropriate scenario.

It is desirable to remove the vertical element (or RL in this case) rapidly but, if this is impossible, the time interval for removing the element should be less than one tenth of the first modal period associated with vertical response of the structural system to the displacement of the reference point at the upper edge of the removed vertical element. This phenomenon is discussed in more detail in [23]. In this paper, the vertical elements were removed abruptly, i.e. in the time interval of Δt = 0.01 s, which is less than one tenth of the period associated with vertical response of the structure to the displacement of the reference point above the removed elements. The analysis of the system

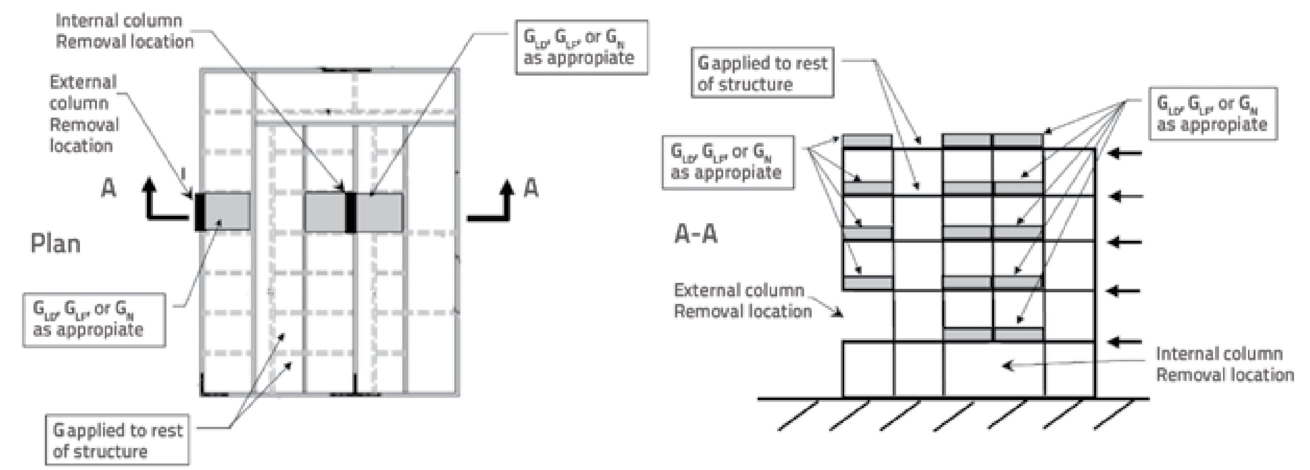

Figure 3. Application of NSA *pushdown* procedure when removing a wall, according to [16]

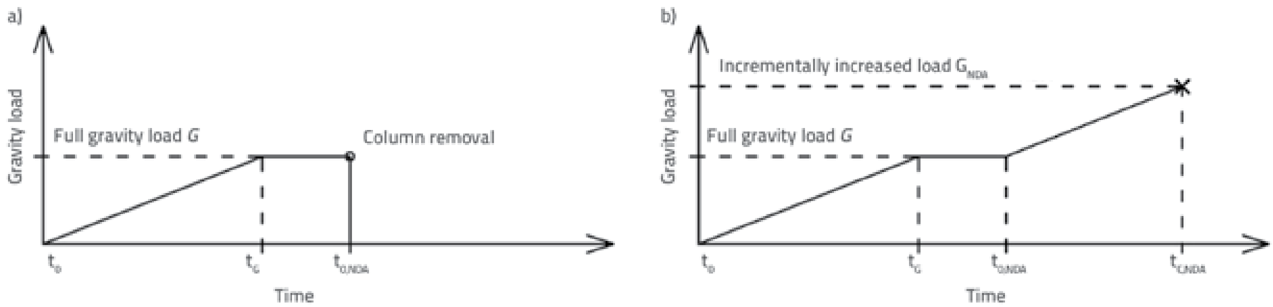

Figure 4. TH functions for applying NDA *pushdown* method

response continues using the combination of loads (2) applied to the entire structural system, with an incremental increase of DIF (Ω) until the maximum displacement of the reference point, or the state of progressive collapse, is reached [15, 16].

Scenarios for the removal of vertical elements at the ground floor and the overall NDA *pushdown* method were performed using *time-history* (TH) functions that are related to the replacement load function (Figure 4a) and the load combination (2) (Figure 4b). The replacement load (RL) consists of reactive forces in the upper node of the removed element. The RL is used to model the undamaged structure in the scenario of "removal" of the vertical element and the NDA *pushdown* method. Instead of physical presence of the element which will be removed according to the corresponding scenario, RL is used as a "replacement" that simulates its physical presence in the model. The TH functions and their corresponding loads are shown in Figure 4. The values t_0 = 5 s, $t_{0,NDA}$ = 7 s were adopted, and $t_{C,NDA}$ is the time required to reach the state of progressive collapse.

2.3.1. Gravity load

The structure is subjected to two different types of vertical loads: weight of structural elements and an additional constant load (G_j), and the live load (Q_i). The value adopted for the additional constant load is g_{add} = 3.0 kN/m² at all floors. The value of live load is q = 2.0 kN/m² [13] for all ceilings, except for the roof plate where the load intensity is equal to q_r = 1.0 kN/m² [13]. The adopted self weight of façade elements installed on all façade beams, except for the roof façade beams, is equal to $g_{f,beam}$ = 10.0 kN/m and $g_{f,wall}$ = 3.0 kN/m. The value of the live load reduction factor is $\psi_{2,i}$ = 0.3 [6].

2.3.2. Seismic action

The structure is designed for proper gravitational and seismic response, based on the linear-elastic theory method using the software package ETABS [71], and according to guidelines given in structural Eurocodes [6, 13, 83, 84]. The Type 1 response spectrum for the category C soil [84], with PGA of $a_g = 0.30 \cdot g$, was used for the design of the structure. The building is designed as a DCH RC structure, with behavioural factors of q = 5.85 in the X direction, in which the structure behaves like a frame system, and q = 4.4 in the Y direction, in which the structure behaves like a wall system. The building is residential and commercial. The adopted value for the damping factor in both directions is 5 %, according to [84]. A more detailed discussion of the structural system damping is given in [23, 60].

2.4. Calculation model

2.4.1. Model for linear-elastic analysis

A spatial (3D) model was used for the calculation and design of the structure in [71]. The following parameters, assumptions, and simplifications were adopted:

- The calculation includes the effects of the second order logic (*P*-Δ);
- The occurrence of cracks in structural elements was included in the calculation with the stiffness reduction of the elements. From the multitude of recommendations contained in various codes for the calculation of RC structures [88], the values given in [89] were selected for all elements. These values correspond to the values [90] recommended for the software package [71].
- The elastic bending stiffness of columns was reduced to 70 % and that of the beams to 35 %;
- The elastic (membrane) bending stiffness of walls was reduced to 35 % in the critical zone (first two floors) and 70 % on the other floors;
- The torsion stiffness of columns and beams and bending stiffness of walls perpendicular to their plane were reduced to 10 % of their elastic stiffness;
- The shear stiffness of columns, beams and walls was reduced to 40 % of their elastic stiffness.
- The elastic stiffness of the RC plate was reduced to 25 %.

2.4.2. Model for nonlinear analysis

In models for post-elastic analysis of structural response to the removal of individual vertical elements, the following assumptions and simplifications were used:

- The calculation includes the effects of the second order logic (*P*-Δ);
- To describe nonlinear behaviour of the material, nonlinear properties of the material were used to describe the behaviour of concrete (Figure 5) [85] and reinforcement steel [83];

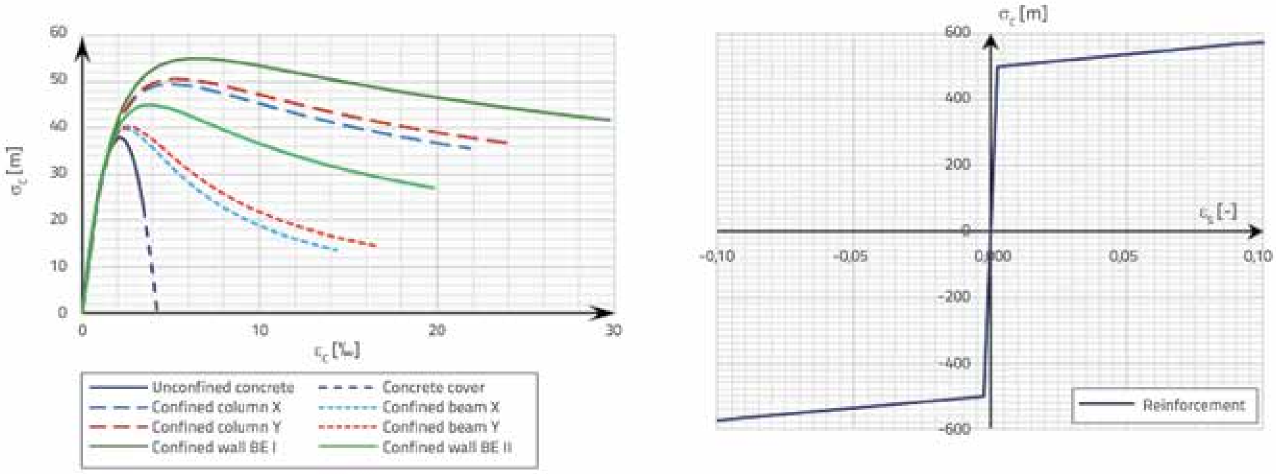

Figure 5. Stress-dilation functions for materials and elements used in nonlinear analysis

- Parameters describing the appearance of cracks in structural elements from the linear-elastic model were not included in the nonlinear model, because plastic hinges are modelled as fibre elements, whereas the properties of fibres are described by stress-strain relations in concrete and reinforcement steel;
- Edge wall elements, columns, and beams were modelled as confined RC elements with a protective layer of concrete [85];
- The behaviour of RC is described by the Takeda hysteretic model, while the Kinematic model of hysteresis was used for reinforcement. Both models are an integral part of the software package [71].

The contribution of the RC plate is included in the calculation model through its corresponding effective widths in the composition of the beams [83], i.e. plates are not treated as surface elements, but within the "T" cross section of the beam. The consequence of this simplification is that the results may indicate lower system robustness than the actual one, but the calculation favours safety.

In addition, in order to compare and evaluate the effect of the plate effective width on progressive collapse, structural robustness was also calculated without the inclusion of plate effective width in the beam cross section.

2.4.3. Properties of plastic hinges

Plastic hinges in beams are modelled as fibre cross sections. Facade beams contain 12 fibres of protective concrete layer and 4 fibres of unconfined concrete (interior of the RC plate), while for internal beams (Figure 6), the number of fibres of protective concrete layer is 16, and the number of fibres of unconfined concrete is 8. All beams contain 32 fibres of confined concrete (beam cores) and the corresponding reinforcement fibres – 5 for beams in the *X* direction and 6 for beams in the *Y* direction, as well as 8 additional reinforcement fibres for each side of the plate effective width. Plastic hinges in walls and columns are modelled by automatic selection of fibre division in the cross section of elements, which makes a total of 107 fibres in wall sections and 31 fibres in facade columns in the Y direction, and 41 fibres in all other columns in the structural system. The

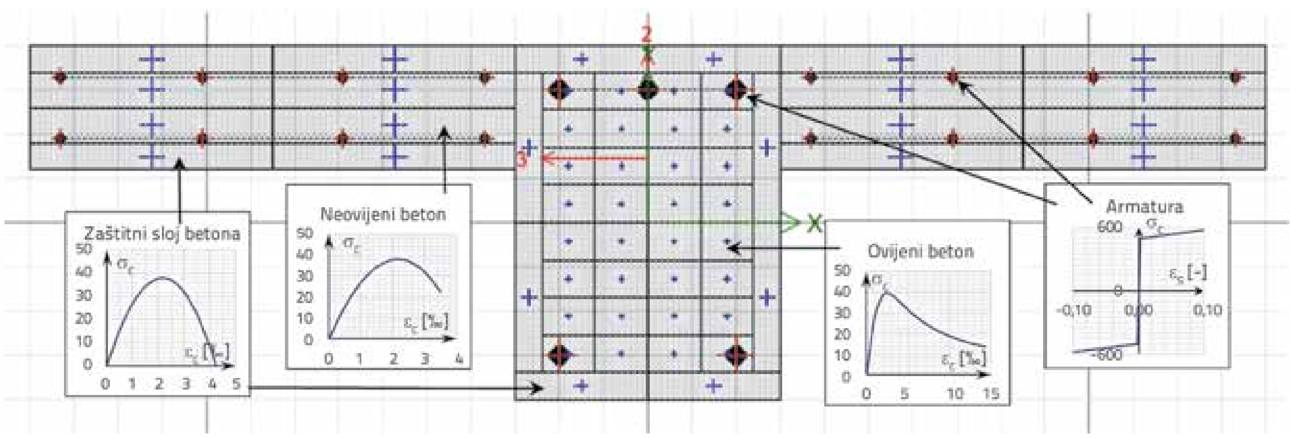

Figure 6. Schematic representation of "T" division of the beam cross section into fibres with appropriate stress state properties depending on material used

reason for the detailed modelling of plastic hinges in beams is that they are, being horizontal elements in the structure, most exposed to capacity loss and collapse due to incremental application of gravity load. Plastic hinge lengths are calculated according to [91].

"Fibre models of plastic hinges are more accurate because the nonlinear material ratio of each fibre is automatically integrated into the interaction, changes along the moment-rotation curve, and the plastic axial stress. The problem with this approach, in plastic hinge modelling is that the use of fibres is computationally more demanding" [92].

3. Results and discussion

3.1. Damping and modal analysis

Rayleigh mass (M) - tangential stiffness (K_T), viscous damping was applied in the NDA (Figure 4). The damping matrix of the system is a combination of the mass and stiffness matrices, as shown in the following equation:

$$[C] = \alpha_M \cdot [M] + \alpha_K \cdot [K_T] \tag{3}$$

where $[C]$, $[M]$ and $[K_T]$ are the damping, mass, and tangential stiffness matrices, respectively. Parameters α_M and α_K represent proportional coefficients of the damping of mass and stiffness, and they are equal to:

$$\alpha_M = 4\pi \cdot \frac{\xi_{1,i} \cdot T_{1,i} - \xi_{2,i} \cdot T_{2,i}}{T_{1,i}^2 - T_{2,i}^2}, \alpha_K = \frac{T_1 \cdot T_2}{\pi} \cdot \frac{\xi_{2,i} \cdot T_{1,i} - \xi_{1,i} \cdot T_{2,i}}{T_{1,i}^2 - T_{2,i}^2} \tag{4}$$

where $T_{1,i}$ and $T_{2,i}$ are the first and the last periods of vibration of interest for the analysis of structural response. $\xi_{1,i}$ and $\xi_{2,i}$ are the corresponding relative damping coefficients with the adopted values of 0.05. The Rayleigh damping function is calculated by applying the expression:

$$\xi_i = \xi_{M,i} + \xi_{K,i} = \frac{\alpha_M}{2 \cdot \omega_i} + \frac{\alpha_M \cdot \omega_i}{2} = \frac{\alpha_M \cdot T_i}{4 \cdot \pi} + \frac{\alpha_K \cdot \pi}{T_i}, \left(\omega_i = \frac{2\pi}{T_i} \right) \tag{5}$$

where ω_i is the angular frequency for the corresponding inherent form of vibration. The value of T_1 is the first vertical period of translation in the *Z* direction, related to the vertical displacement of the upper node of the removed element. The value of T_2 is the vertical translation period in the Z direction, which refers to vertical displacement of the upper node of the integrated element in which the structural system reaches at least 90 % of the sum of effective modal masses in the *Z* direction. The values of periods used are shown in Table 2.

In the first case, without inclusion of the RC plate effective width in the calculation model, the ratio of vibration period values, from the lowest to the highest, can be described as follows: A3 < C1< C3 < C2 < B3 < B1 < B2 < W1. In the second case, with inclusion of the plate effective width in the calculation model, the ratio of vibration period values, from the lowest to the highest, can be described as follows: C3 < C2 < C1 < A3 = B3 < B2 < B1 < W1. In both cases, vibration period values in the case of removal of wall *W1* are significantly higher than vibration period values in the case of removal of columns.

3.2. Influence of removal of vertical elements on structural system

Figure 7 shows vertical displacements of the upper nodes of the removed columns, with a time increment of Δt = 0.01s in the case of the column removal scenario ($t_{0,NDA}$) (Figure 3, left). There is a noticeable difference in deflection between the beam system in which the influence of the plate effective width (left) is excluded, and the system in which it is included (right). Initial values of deflection after element removal are expected to be higher in the first case (left). Also, the inclusion of the plate effective width in cross sections of façade beams (one-sided) and inner beams (two-sided), which contributes to the reduction of vertical deformations, also results in different ratios of deflection values for different scenarios when comparing the first (left) and the second case (right).

In the first case (Figure 7, left), without inclusion of the plate effective width in calculation model, the displacement values, from the lowest to the highest, after the system "calms down", can be described as follows: A3 < C1< C3 < C2 < B3 < B1 < B2 < W1. In the second case (Figure 7, right), with inclusion of plate effective widths in calculation model, the displacement values from the lowest to the highest after

Table 2. First and last relevant vibration periods for the NDA system

Element notation	Without plate effective width		With plate effective width	
Vibration period [s]	T_1	T_2	T_2	T_2
W1	3.212	0.023	0.371	0.020
B1	0.273	0.022	0.209	0.020
C1	0.212	0.022	0.182	0.020
B2	0.326	0.022	0.196	0.020
C2	0.224	0.021	0.172	0.020
A3	0.210	0.022	0.185	0.020
B3	0.233	0.022	0.185	0.020
C3	0.220	0.021	0.165	0.020

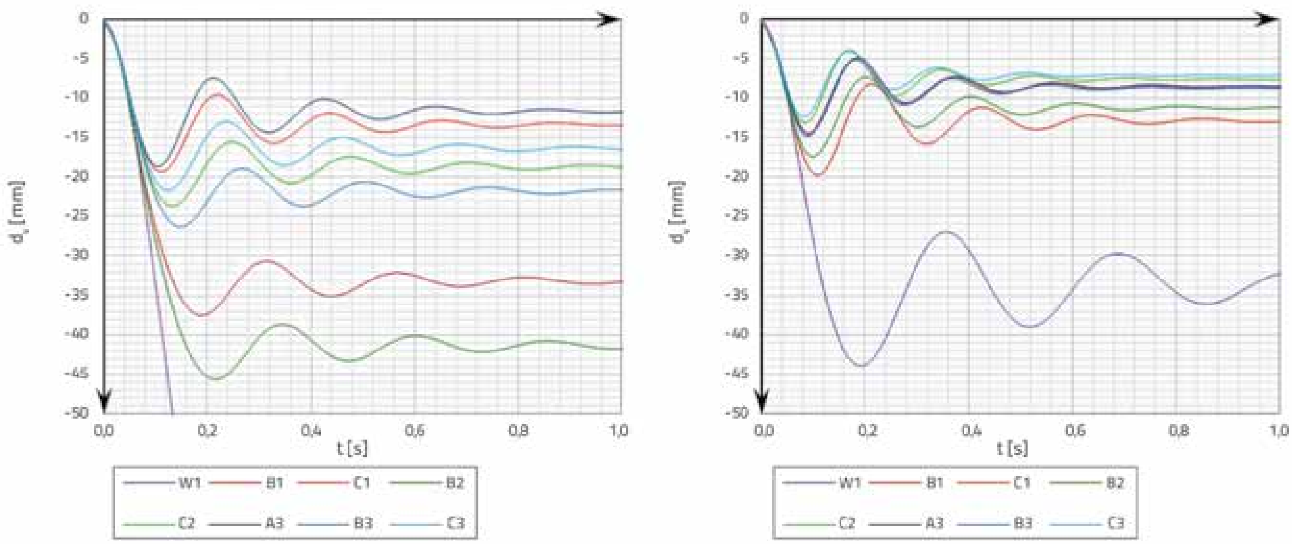

Figure 7. Vertical displacements of the upper points of the removed vertical element: without inclusion of plate effective width (left), with inclusion of plate effective width (right)

the system "calms down" can be described as follows: C3 < C2 < A3 < C1 < B3 < B2 < B1 < W1, where the difference in the amount of displacement between the elements A3, C1, and B3 is negligible. In both cases, reference point displacement values in the case of removal of wall W1 are significantly higher than the corresponding values in the case of removal of columns.

In the first case (Figure 7, left), maximum displacement values due to column removal range from 18.58 mm to 45.58 mm, while displacement values after the system "calms down" vary from 11.65 mm to 41.35 mm. In the second case (Figure 7, right), maximum displacement values due to column removal vary from 12.37 mm to 19.78 mm, while the displacement values after the system "calms down" vary from 7.13 mm to 12.88 mm. In the first case, the progressive collapse of the edge part of the structural system will occur after wall removal. In the second case, after wall removal, the maximum displacement value is 43.90 mm, while the displacement value after the system "calms down" is 33.67 mm.

3.3. Nonlinear pushdown analysis

Analyses based on the NSA and NDA methods were performed according to provisions given in references [15, 16], while the method used for loading the damaged structure model is described in detail in Section 2.3. Using these methods, the post-elastic behaviour of the system, depending on the adopted damage scenarios, was analysed. For the adopted scenarios, the relations between the structural capacities to resist progressive collapse were analysed, depending on whether the plate effective width is included in the models or not. The pushdown analysis results are shown in Figure 8.

As expected, the ratio of *pushdown* functions, i.e. the capacity of the structure to resist progressive collapse, corresponds to the results and the ratio determined by the analysis of the effects of vertical element removal on vertical displacement of the reference point.

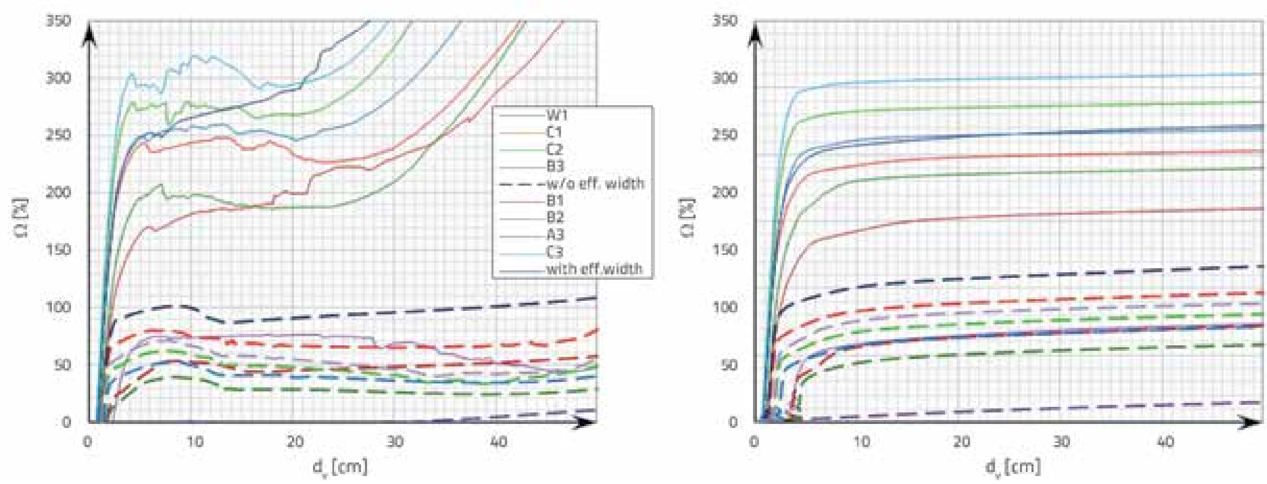

Figure 8. Results of *pushdown* analysis obtained using NSA (left) and NDA (right)

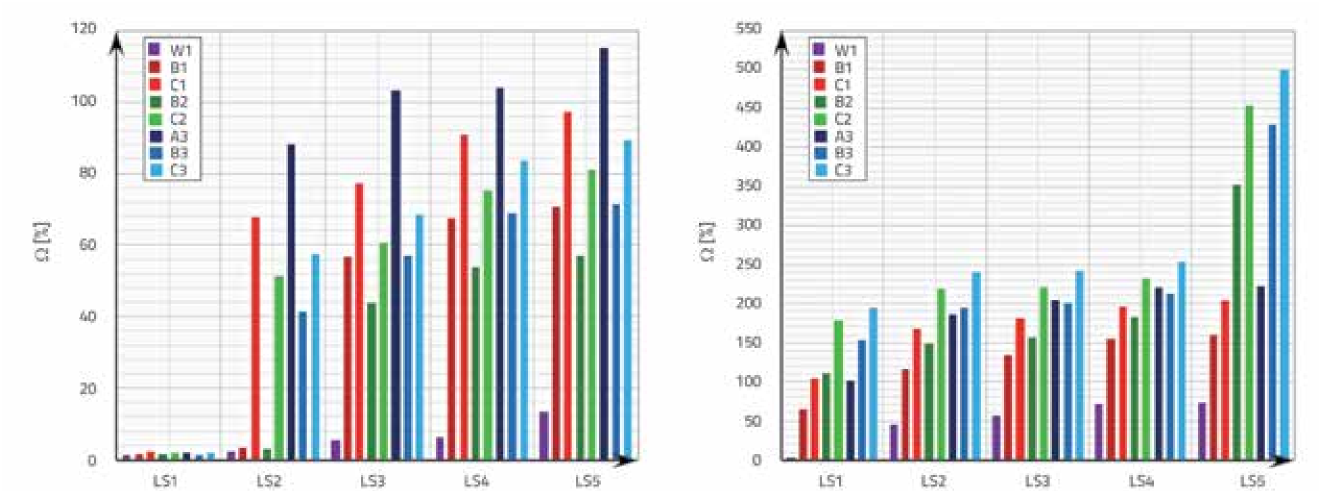

Figure 9. DIF (Ω_i) values depending on damage limit states of the system (*LSi*): without inclusion of the plate effective width (left), with inclusion of the plate effective width (right)

It is obvious that the capacity of the structural system is much higher in the second case than in the first case of system modelling. This difference can clearly be seen in Figure 8. In addition, the expressed fragility of the system to wall removal is obvious compared to the removal of other elements (columns).

In the first case, without inclusion of the plate effective width in the calculation model, the robustness of the system obtained by applying the NSA method (Figure 8, left) from the lowest to the highest, from the aspect of DIF (Ω), can be described as follows: A3 > C1 > C3 > C2 > B3 > B1 > B2 > W1, which also corresponds to the value interrelation obtained by applying the NDA method (Figure 8, right). In the second case, with inclusion of plate effective widths in the calculation model, the robustness of the system obtained by applying the NSA method (Figure 8, right) from the lowest to the highest, from the aspect of DIF (Ω), can be described as follows: C3 > C2 > C1 > A3 ≈ B3 > C1 > B2 > B1 > W1, which also corresponds to the value interrelation obtained by applying the NDA method (Figure 8, right). Also, in both cases, the robustness of the system in the case of the removal of wall W1 is significantly less than the robustness of the system in the case of the removal of columns. In addition to the above, a slightly higher capacity of the system with regard to progressive collapse can be observed after inclusion of the plate effective width in the calculation model, when applying the NSA method (Figure 8, left) compared to the NDA method (Figure 8, right).

3.4. Damage limit states

The methods proposed in [77, 78] were used in order to quantify and compare column removal scenario results from the aspect of the risk of progressive collapse of the structure. Damage limit states (LS) of the structure were determined for the results obtained using the NDA method. Damage limit states were defined on the basis of recommendations proposed in [61], depending on the values of dilatations of the beam material running in the *X* and *Y* directions, as follows:

State LS1 (minor damage): Depends on steel and concrete values. LS1 occurs either in the first step, when reaching the reinforcement creep limit (ε_{ys} = 2.5 ‰) [83] or the stress limit of concrete with maximum strength in the protective layer of concrete (ε_{c1} = 2.16 ‰) [85].

State LS2 (moderate damage): Occurs when the vertical displacement, obtained as the ratio of displacement of the top above the removed column and the length of the beam span, exceeds the determined threshold $D_{r,vert}$ = 1.0 % [61].

State LS3 (significant damage): This level of damage is assumed to occur when reaching the stress limit in the protective layer of concrete (ε_{cu1} = 4.2 ‰) [85] or the maximum stress of the confined concrete core ($\varepsilon_{c1,cXdir}$ = 2.45 ‰, $\varepsilon_{c1,cYdir}$ = 2.62 ‰).

State LS4 (severe damage): Occurs in the first step, when the ultimate stress is reached in the confined concrete core ($\varepsilon_{cu,cXdir}$ = 14.33 ‰, $\varepsilon_{cu,cYdir}$ = 16.71 ‰) [91].

State LS5 (progressive collapse): This state results in the case of tensile fracture of longitudinal reinforcement bars (ε_{yu} = 10 %), the end vertical drift of the beam in the floors above the removed column ($\theta = \theta_u$) with the loss of system balance or lack of numerical convergence. In this paper, LS5 was determined as the state at the dilatation value in steel at which tensile fracture in the longitudinal reinforcement bar occurs [83].

Figure 9 shows damage limit states caused by removal of the corresponding vertical elements, without the influence of the plate effective width (left) and with the influence of the plate effective width (right). There is a big difference between the bearing capacity of beams in the first (left) and second (right) case, which certainly corresponds to the tendencies observed in previous analyses.

The ratio of damage limit states corresponds to the results presented so far and to their ratio. In the first case, without inclusion of the plate effective width in the calculation model, the response of the structure in the form of reaching the damage limit states from the most favourable to the most unfavourable, can be described as follows: A3 > C1 > C3 > C2 > B3 > B1 > B2 > W1. In the second case, with inclusion of plate effective widths in the calculation model, the response of the structure from the aspect of reaching the damage limit states from the most favourable to the most unfavourable can be described as follows:

$$C3 > C2 > \begin{matrix} B3 > A3 \text{ (za LS1 i LS2)} \\ A3 > B3 \text{ (za LS3 i LS4)} \end{matrix} > C1 > B2 > B1 > W1,$$

except in the case of state LS5 where the entire bearing capacity is transferred to the reinforcement up to the point of reaching its limit dilatation, after which the state of progressive collapse occurs. In this case, the damage limit state LS5 from the most favourable to the most unfavourable can be described as follows: C3 > C2 > B3 > B2 > A3 > C1 > B1 > W1.

Figure 10 shows mean values of structural damage limit states caused by removal of the corresponding vertical elements, without inclusion of the plate effective width (Figure 10, left) and with inclusion of the plate effective width (Figure 10, right). There is a big difference between the bearing capacity of beams in the first and second case, and it is higher in the second case.

The bearing capacity of beams modelled with inclusion of the plate effective width (Figure 9, right) contributes to a higher structural system robustness compared to the models in which the RC plate effective width is not taken into account (Figure 9, left). From the state LS1 to the state LS4, which are dependent on dilatations in concrete at yield strength of reinforcement, the difference in system capacity

$$\Delta\Omega_{LSi} = \Omega_{LSi}^{with\ eff.\ width} - \Omega_{LSi}^{w/o\ eff.\ width}$$

before reaching the corresponding damage state varies from 111.85 % to 125.22 % of the dynamic increase factor (DIF) of the gravity load acting on the system (Figure 10). The effect of modelling beams with inclusion of the RC plate effective width on the increase in the system's bearing capacity is obvious. In the case of state LS5, which depends on reaching the limit tensile stress in the reinforcement, this difference is slightly higher and amounts to 225.10 % (Figure 10), which makes the beam cross-section modelling, with and without inclusion of plate effective width, the most influential factor.

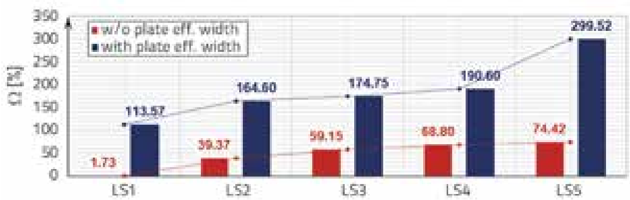

Figure 10. Mean values of damage limit states (*LSi*)

High DIF values in the second case with LS5 (Figure 9, right) also follow the number of beams that are joined above the removed element, i.e. the DIF value for LS5 is significantly higher in cases when four beams are joined in the node at the location of the removed element, compared to three beams in other scenarios. This phenomenon is characteristic of the second case (Figure 9, right), where the plate effective width is included in calculation and does not apply to the first case (Figure 9, left), where the plate effective width is not included. In the first case (Figure 9, left), the most resistant systems are those in which a smaller number of beams are joined in the node of the removed element, at a greater distance from the edge of the system at the base (A3 and C1). The same cannot be said for the case of the column B1 removal, where the system exhibits less robustness. Also, unlike the second case, there is no effect of "T" and "L" beam cross-section, which increase the capacity to accept pressure stress in the upper beam zone at the reference points (at the location of the removed element), nor additional reinforcements in the effective part of the plate that increases the capacity to absorb tensile stress in the upper beam zone at the other end of the span (relative to the point of the removed element). In addition to the above, one of the very important factors that depends on the system robustness is the influence of position of the removed vertical element in relation to the centre of stiffness of the structure, which is discussed in Section 3.6.

3.5. Calculation of fragility curves

Based on damage limit state calculation results, the method of mathematical probability and statistics was applied for the purpose of calculating and constructing functions of fragility curves. In this way, results of the scenario of removing vertical elements of the structure in the ground floor were quantified and compared from the perspective of probability of occurrence of different degrees of system damage.

According to [9] "fragility functions can be defined as mathematical functions that express the probability of an adverse event to occur. The fragility function is the cumulative distribution of the function of capacity of a structural system to resist an undesired limit state."

Fragility functions are functions of dependence of the intensity measure (IM) and the probability of exceeding a certain limit state of structural damage. The use of a log-normal, normal, or uniform distribution function is the most appropriate in seismic engineering and fragility analysis [9]. Based on the software package [93], and the Kolmogorov-Smirnov and Anderson-Darling tests, it was found that the application of the normal distribution function is more suitable for the construction of fragility curves:

$$f(\Omega_i) = \frac{1}{\sigma_{LSi} \cdot \sqrt{2\pi}} \cdot e^{-\frac{1}{2}\left(\frac{\Omega_i - \mu_{LSi}}{\sigma_{LSi}}\right)^2} \tag{6}$$

where μ_{LSi} and σ_{LSi} represent parameters of the mean value and standard deviation value of the corresponding damage limit state LSi. The probability of occurrence of the corresponding damage limit state (LSi) for the DIF (Ω_i) value is calculated by applying the analytical cumulative distribution function (CDF) for normal distribution:

$$P_{LSi}\left[\Omega_i, \mu_{LSi}, \sigma_{LSi}\right] = \Phi\left(\frac{\Omega_i - \mu_{LSi}}{\sigma_{LSi}}\right) \tag{7}$$

where Φ is the CDF for the standard normal distribution function. The ratio of probability of occurrence of damage limit states is clearly defined as:

Table 3. Statistical parameters for constructing fragility curves

Distribution parameters	Without plate effective width				With plate effective width			
Damage limit state	μ_{LSi}	σ_{LSi}	$\sigma_{LS,C1}$	$\sigma_{LS,C2}$	μ_{LSi}	σ_{LSi}	$\sigma_{LS,C1}$	$\sigma_{LS,C2}$
LS1	1.725	0.282		1.,448	113.575	62.724		62.724
LS2	39.375	33.058		33.058	164.600	62.188		62.188
LS3	59.150	27.939	30,579	30.772	174.750	58.865	95,878	60.738
LS4	68.800	29.569		29.700	190.600	56.944		58.475
LS5	74.425	30.463		30.463	299.525	155.564		91.893

$$P_{LS1}(\Omega_i) > P_{LS2}(\Omega_i) > P_{LS3}(\Omega_i) > P_{LS4}(\Omega_i) > P_{LS5}(\Omega_i) \qquad (8)$$

When constructing system fragility curves, it is common for certain fragility functions to "intersect" for various damage states, i.e. deviations from expression (8) can occur. The solution is considered in [9] and it is based on the adoption of a common parameter $\sigma_{LS,C1}$ for all damage limit states. In this paper, the *Maximum Likelihood Estimation* (MLE) method was applied [9, 94]. The condition (8) is satisfied, but some deviations of results relating to uncorrected values (Figure 11, left and Figure 12, left) can be further reduced. This can be achieved by correcting parameters σ_{LSi}, so that the corrected values $\sigma_{LSi,C2}$ can be determined as values with the lowest deviation from the calculated values of σ_{LSi}, while maintaining the order (8). The

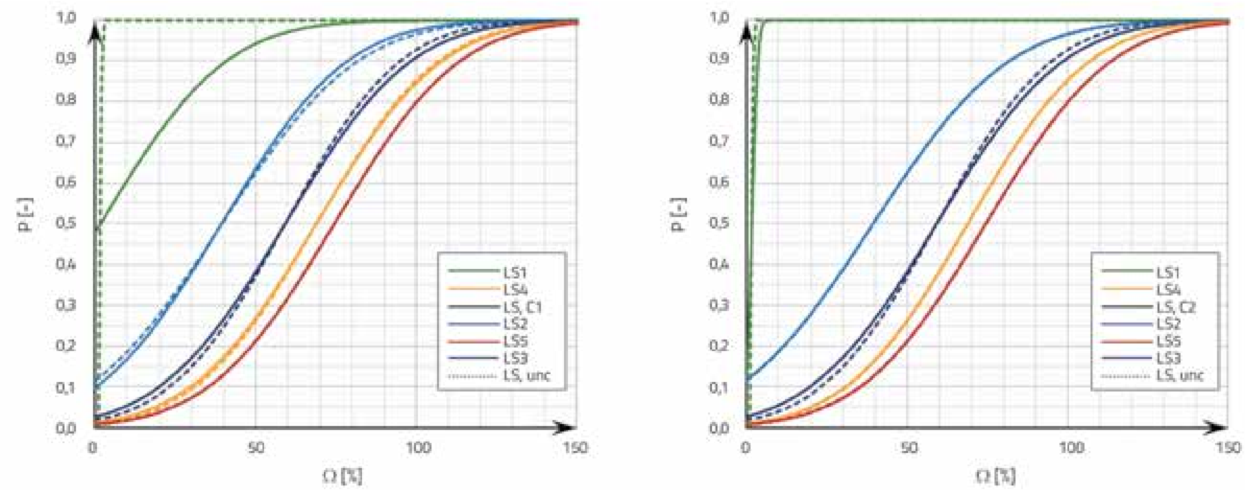

Figure 11. Fragility curves (without the inclusion of the plate effective width): according to [9] ($P_{LSi,C1}$) (left), minimum corrections of standard deviation ($P_{LSi,C2}$) (right)

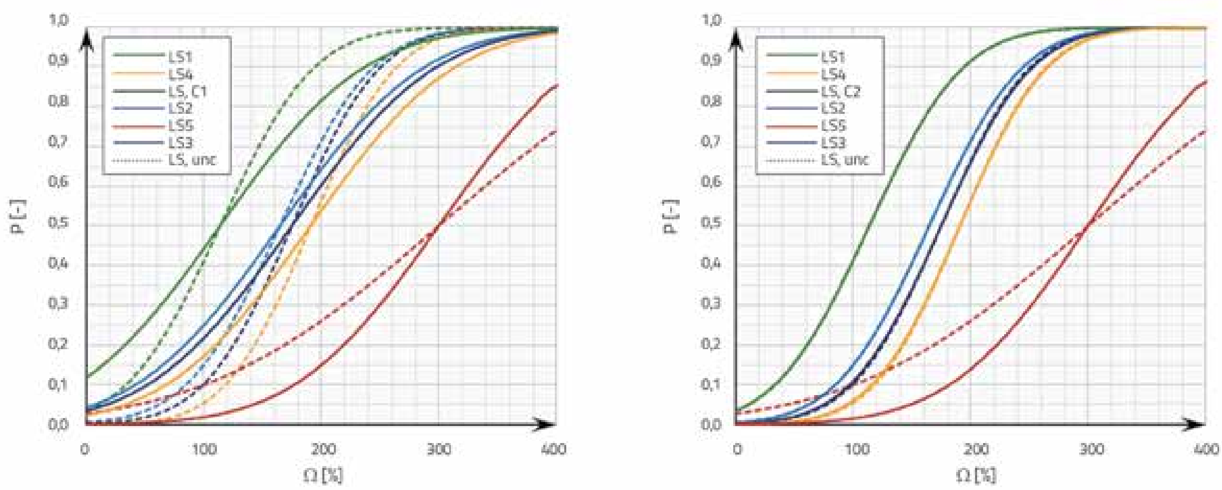

Figure 12. Fragility curves (with the inclusion of plate effective width): according to [9] ($P_{LSi,C1}$) (left), minimum corrections of standard deviation ($P_{LSi,C2}$) (right)

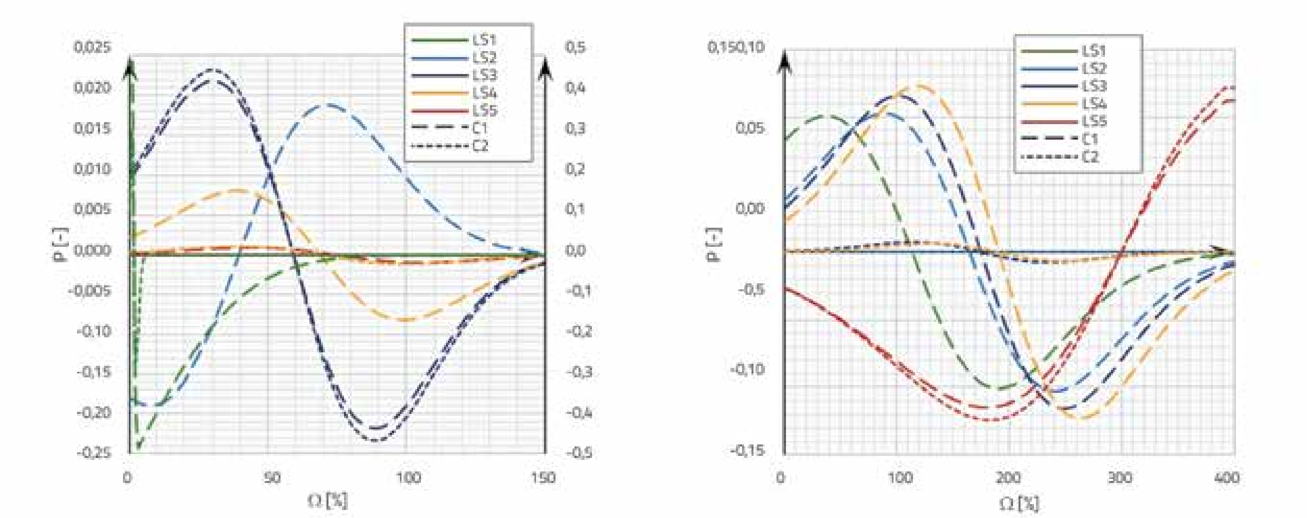

Figure 13. Deviation values of corrected fragility functions: without inclusion of plate effective width (left), with inclusion of plate effective width (right)

response parameters μ_{LS}, σ_{LS}, $\sigma_{LS,C1}$ and $\sigma_{LS,C2}$ of the structural system to the progressive collapse from the aspect of the damage limit states are shown in Table 3.

Figures 11 and 12 show fragility curves without inclusion of the plate effective width. Figures 11 and 12 (left) show fragility functions obtained using the procedure described in [9] ($P_{LSi,C1}$), while fragility functions in Figures 11 and 12 (right) are calculated using an iterative procedure $P_{LSi,C2}$, so that values of the corresponding standard deviations have a minimum deviation from uncorrected values ($P_{LSi,unc}$), meeting the condition (8).

Figure 13 shows deviations corrected from originally calculated fragility functions, according to the expression:

$$\Delta P_{LSi} = P_{LSi,Cj} - P_{LSi,unc};\ (i = 1, 2, 3, 4, 5),\ (j = 1, 2) \tag{9}$$

It is necessary to mention that very high values of deviation were obtained for meeting the condition (8) for state LS1 (without inclusion of plate effective width). In the case of the first method (C1), this value reaches a deviation of less than 1 % from the uncorrected values only at Ω = 80 %, while in the case of the second method (C2), the deviation value for LS1 reaches a value of less than 1 % from the uncorrected values already at Ω = 6 % (Figure 13, left), which points to higher accuracy of the second method (C2).

When applying both methods (with inclusion of the plate effective width), the maximum value of deviation of the results in relation to the uncorrected fragility function for LS5 (Figure 13, right) is ± 11.49 % (C1) and ± 12.45 % (C2), respectively. Higher deviation values are the result of satisfying condition (8).

It can be observed that the deviation values are in most cases lower when the second result correction method (C2) is applied, that is, it can be concluded that the results obtained using the second correction method (C2) are more accurate in describing probability of different damage limit states.

Table 4. Deviations of corrected fragility functions from uncorrected fragility functions

Deviation values	Without plate effective width		With plate effective width	
Damage limit state	C1	C2	C1	C2
LS1	± 48.55 %	± 30.33 %	± 10.12 %	± 0.00 %
LS2	± 1.89 %	± 0.00 %	± 10.31 %	± 0.00 %
LS3	± 2.18 %	± 2.34 %	± 11.57 %	± 0.75 %
LS4	± 0.81 %	± 0.11 %	± 12.32 %	± 0.64 %
LS5	± 0.09 %	± 0.00 %	± 11.49 %	± 12.45 %

3.6. Effects of position of removed element on limit states of system damage

The results of previous analyses show a clearly less favourable response of the system in which the beams were modelled without inclusion of the plate effective width, compared to the system in which the beams were modelled with inclusion of the plate effective width. In addition, there is a difference in the resistance of the structure to reaching certain limit states depending on the position of removed element in the structural system.

In the first case (Figure 9, left), the system has the highest resistance to progressive collapse when facade columns A3 (smaller cross section than others, Table 1) and C1 are removed (these columns are also the furthest facade columns from the edge of the building at the base). They are followed by the inner columns C3 and C2, which are also the furthest innermost columns from the edge of the building at the base. They are followed by the façade column B1, equally distant as C2 from the edge of the system at the base, but at a distance of one span from the column presenting the smallest dimensions. This is followed by columns B1 and B2 whose associated beams rely on the RC wall. The system is the weakest when removing the wall W1,

Table 5. Distance of columns from the centre of stiffness of the system

Removed element	C3	C2	B3	B2	A3	C1	B1	W1
D_c - Distance from CoS-a [m]	2.97	6.64	6.64	8.91	10.71	10.71	12.24	13.45

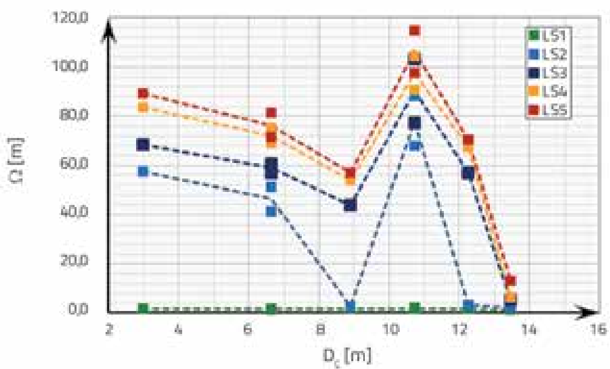

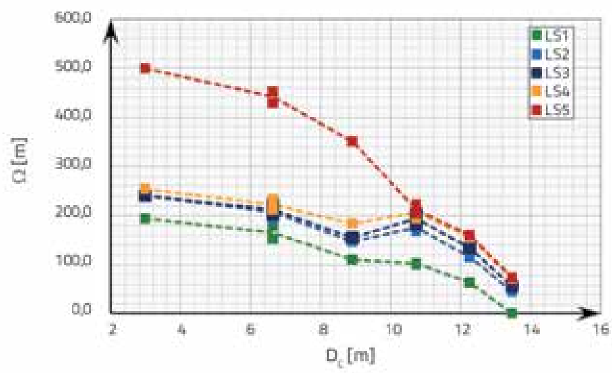

Figure 14. Influence of the distance of the removed element from the centre of the system rigidity on the damage limit states: without the inclusion of the plate effective width (left), with the inclusion of the plate effective width (right)

located at the very edge of the building at the base, which results, as already mentioned, in progressive collapse.

In the second case (Figure 9, right), the system has the highest resistance to progressive collapse when removing the inner columns C3 and C2, which are also the furthest inner columns from the edge of the building at the base, and the closest to the centre of stiffness of the system. They are followed by internal column B3, equally distant as C2 from the edge of the building at the base, but at a distance of one span from the column of the smallest dimensions. This is followed by an inner column B2 whose associated beam is supported by and extended perpendicular to the RC wall. This is followed by facade column A3 (smaller cross-section compared to the others, Table 1), and then by facade columns C1 and B1. The system is the weakest after removal of wall W1 located at the very edge of the building at the base. The centre of stiffness (CoS) of the system is located in the very centre of the section at the base, because the structure is biaxially symmetrical. Figure 14 shows the influence of distance of the removed elements from the CoS on their resistance to progressive collapse from the aspect of DIF (Ω). Distance of the columns from the CoS is shown in Table 5.

While in the first case (Figure 14, left) there is no clear dependence between Ω and CoS, in the second case, it is very clear and there is a noticeable tendency towards decreasing system robustness as the distance of the removed element from CoS increases. In the second case, it can be said that system robustness is inversely proportional to the distance of the removed vertical element from the CoS.

4. Conclusions and recommendations

Since buildings cannot be designed for every hazard to which the structural system may be exposed during its lifetime, a general design approach should take into account the action associated with low probability events and huge consequences for the structural system, which is characteristic of progressive collapse [7]. It is very important to provide a reserve capacity for nonlinear system behaviour and force redistribution. Such behaviour essentially depends on ductility and detailing of the elements and on their interconnections, as well as on the ability of the structure to develop an alternative load transfer path in the event of loss of a vital element. In addition, to ensure that the elements can act together, an adequate continuity of ductility of joints and reserves of bearing capacity should also be ensured – higher static uncertainty, i.e. (redundancy) [7]. Structures designed in accordance with recommendations for seismically resistant buildings show lower fragility than those that are not designed in accordance with seismic regulations [77]. After a column is removed, a beam with a double span is formed, so that the lower and side reinforcement should be continued, which is necessary in seismically active areas. A number of documents and codes contain recommendations for the calculation of structures that are less susceptible to progressive collapse, i.e. robust structures. Structural design regulations should focus on guidelines that are aimed at achieving a sufficient level of system resistance to progressive collapse.

This paper analysed the robustness, i.e. the capacity of a five-storey RC building to resist progressive collapse. Nonlinear analysis methods (NSA and NDA) were used to analyse robustness of the structure. The structural response for the scenarios of loss of one vertical element on the ground floor (column or wall) was analysed. The results of NSA and NDA application are presented in the form of pushdown curves. More precisely, the states of damage limit of the system were determined by applying the NDA method based on the stress-strain states of the material, according to [61]. Using the methods of mathematical statistics and probability, fragility curves of the RC building were constructed and probabilities for the occurrence of damage limit states were obtained.

- Two approaches in beam element modelling were compared:
- without inclusion of the plate effective width
- with inclusion of the plate effective width, and comparing the results.

From the obtained results, it can be concluded:
- The first and last relevant vibration periods related to translation of reference points in the *Z* direction are higher in the first case, which is expected, since the system has a higher vertical stiffness in the second case.
- Effects of removal of vertical elements, from the aspect of magnitudes of vertical displacements of the reference point, are also better absorbed by the system in the second case.
- The results of modal, *pushdown* analysis, calculation of fragility limit states, as well as calculation of fragility curves, indicate a much more pronounced measure of system robustness in the second case than in the first case of structural modelling.
- In addition, by comparing the results of the analysis, the following was concluded:
- There is a pronounced fragility of the structural system to the loss of the wall compared to the loss of columns. It was found that in the first case of system modelling, when the wall is lost, there is a progressive collapse of that part of the system.
- Although the application of both methods to correct the intersecting fragility curves leads to certain deviations from the uncorrected values, the application of the second correction method (C2) provided results of higher accuracy.
- It was found that robustness of the structural system decreases with the distance of the removed vertical element from the centre of stiffness of the system, i.e. that the system is most susceptible to progressive collapse when removing the edge and facade vertical elements.

Based on the derived conclusions, it is recommended that the second method of system modelling be applied in the analysis of robustness of RC spatial models, i.e. that the plate effective width be included in the calculation, because it leads to an irrational solution.

The loss of bearing capacity of edge and facade vertical elements contributes the most to the decline in robustness of the system, and so it is necessary to ensure the continuity of the structure and to increase the bearing capacity of joints.

The method proposed in [9] (C1) can be applied when intersection occurs between fragility curves during their construction. In the case of large deviations in the probability of occurrence of certain damage limit states of the system, the second approach (C2) should be used with an iterative procedure of individual corrections of standard deviation values.

When designing the system, it is very important to reduce the exposure of RC walls to the potential danger of losing their bearing capacity, which can be ensured by positioning them in places where they are less exposed to accidental effects of another nature. It is also important to consider an increase in the resistance of RC walls, which are most exposed to accidental actions. Further studies should also focus on the robustness of systems designed according to [84] for high ductility class with different arrangement of RC walls.

Acknowledgement

The research described in this paper was financially supported by the Ministry of Education and Sciences of the Republic of Serbia within the Project: "A comprehensive approach to improvement of interdisciplinary researches in construction education and science" (University of Novi Sad, Faculty of Technical Sciences, Department of Civil Engineering and Geodesy). This support is gratefully acknowledged.

REFERENCES

[1] Adam, J.M., Parisi, F., Sgaseta, J., Lu X.: Research and practice on progressive collapse and robustness of building structures in the 21st century, Engineering Structures, 173 (2018), pp. 122-149

[2] Janssens, V., O'Dwyer, D.W.: Disproportionate collapse in building structures, 2010,

[3] Wang, H., Zhang, A., Li, Y., Weiming, Y.: A Review on Progressive Collapse of Building Structures, The Open Civil engineering Journal, 8 (2014), pp. 183-192

[4] US Dep. of Housing and Urban Development, Portland Cement Association, Skokie, Philosophy of Structural Response to Normal and Abnormal Loads. Report 2, Illinois, USA, 1976

[5] Lind, N.: Tolerable risk , Proc. Int. Conf. on Safety, Risk and Reliability in Eng., 1 (2001), pp. 123-128.

[6] CEN, EN 1990: Basis of structural design, 2002 and Designers' Guide to EN 1990, Thomas Telford, 2002.

[7] Folić, R.: Structural Robustness of Monolitic and Precast RC structures, Plenary lecture, Reinforced Concrete and Masonry Structures - Theory and Practice, 22-23 October 2015, Sofia, Bulgaria, Book of Abstracts, pp. 18, Full paper electr. pp. 37 – 54. http://www.rc-structures.bg/

[8] Brunesi, E., Parisi, F.: Progressive collapse fragility of European RC buildings, 13th Intern. Conf. On Appl. And Probab. In Cvil Eng. ICASP 13, Seoul, S. Korea, May 26-30 2019, pp. 1-9

[9] Porter, K.: A Beginner's Guide to Fragility, Vulnerability, and Risk. University of Colorado Boulder, 2020, https://www.sparisk.com/pubs/Porter-beginnersguide.pdf

[10] American Society of Civil Engineers (ASCE), Standard ASCE/SEI 41-17, Seismic Evaluation and Retrofit of Existing Buildings, 2017

[11] Brooker, O.: How to design concrete buildings to satisfy disproportionate collapse requirements, The Concrete Centre, Ref:TCC/03/45, October 2008

[12] Woliński, S.: Defining of the structural robustness, Bulletin of the Polish Academy of Technical Sciences (CE), 61 (2013) 1, pp. 137-134, Https://doi.org/10.2478/bpasts-2013-0012

[13] CEN, EN 1991, Actions on structures - Part 1-7: General actions - Accidental actions, 2006.

[14] Starossek, U., Haberland, M.: Measures of Structural Robustness – Requirements & Applications, ASCE SEI 2008 Structures Congress, CB, Vancouver, Canada, April 24-26, 2008, pp. 1/10-10/10

[15] GSA, Alternate Path Analysis and Design Guidelines for Progressive Collapse Resistance, October 24, 2013; Revision 1, January 28, 2016.

[16] DoD UFC Guidelines. Design of Buildings to Resist Progressive Collapse, Unified Facilities Criteria (UFC) 4-023-03. Department of Defence (DoD), 2013.

[17] Unified Casualties Criteria (UCF 4-023-03): Design of buildings to resist progressive collapse, June 2017.

[18] COST Action TU0601 – Robustness of Structures – Structural robustness design for Practicing engineers, Sept. 2011. http://www.cost-tu0601.ethz.ch

[19] CPNI – Centre for Protection of National Infrastructure. Review of international research on structural robustness and disproportional collapse, Arup, Department for Communities and Local Government, October 2011.

[20] Giuliani, L.: Structural integrity: robustness assessment and progressive collapse susceptibility, Doct. Dissertation, University di Roma, 2008

[21] Baker J., Schubert, M., Faber, M.: On the assessment of robustness, Structural Safety, 30 (2008), pp. 253–267

[22] Brett, C., Lu, Y.: Assessment of robustness of structures: Current state of research, Front. Struct. Civ. Eng., 7 (2013) 4, pp. 356–368

[23] Kasinos, S., Palmeri, A.: Robustness assessment using nonlinear analysis methods: a parametric study. IN: Topping, B.H.V. and Ivanyi, P. (eds.), Proceedings of the Twelfth International Conference on Computational Structures Technology. Stirlingshire, UK: Civil-Comp, Paper 42, 2014, https://doi.org/10.4203/ccp.106.42

[24] Beck, A.T. et al. A comparison between robust and risk-based optimization under uncertainty, Struct. Multidisc. Optim., 52 (2015) 3. Https://doi.org/10.1007/s00158-015-1263-9

[25] Ellingwood, B.R.: Strategies for mitigating risk of progressive collapse, ACSE Structures Congress 1, 5-6 2005.

[26] Iribarren, B. S.: Progressive collapse simulation of RC structures: influence of design and material parameters and investigation of the strain rate effects, Univ. Of Bruxelles, Doctor. Diseration , 2011.

[27] Choi, H., Kim, J.: Progressive collapse-resisting capacity of RC beam-column sub-assemblage, ICE Magazine of Concrete Research, 63 (2011) 4, pp. 297-310

[28] Yu, J., Tan, K.H.: Numerical analysis with joint moddel on RC assemblages subjected to progressive collapse, ICE Magazine of Concrete Research, 66 (2014) 23, pp. 1201-1218, https://doi.org/https://doi.org/10.1680/macr.14.00100

[29] Herraiz, B., Russell, J., Vogel, T.: Energy-based method for sudden column failure scenarios: theoretical, numerical and experimental analysis, IABSE Workshop Helsinki, 2015, https://doi.org/10.3929/ethz-a-010389549

[30] Xu, G., Ellinwood, B.R.: A energy-based partial pushdown analysis procedure assessment of disproportional collapse potential, Journal of Steel Research, 67 (2011), pp. 547-555.

[31] Dusenberry, D.O., Ronald, O, Hamburger, S.E.: Practical means for energy-based analyses of disproportionate collapse potential, ASCE J. of Performance of Constructed Facilities, 20 (2006) 4, pp. 336-348

[32] fib (CEB-FIP) Bulletin 66: Model Code 2010, Final draft, 2 (2013).

[33] Folić, R., Lađinović, Đ., Zenunović, D.: Robustness versus progressive collapse of RC buildings, Abstract, p. 59. Paper on CD ROM, 249-258. Https://doi.org/10.14415/konferencijaGFS2014, April 2014, Subotica

[34] Ameri, M.R., Massumi, A., Masoomi, H.: Effect of Structural Redundancy on Progressive Collapse Resistance Enhancement in RC Frame Structures, ASCE J. Perform. Constr. Facil., 33 (2019) 1

[35] Arhain, A.H., Morgenthal, G.: Alternative path sensitivity analysis nof RC frames using First-order seconnd moment method, IABSE Workshop Helsinki, 2015, pp. 170-177.

[36] Fascetti, A., Sashi, K., Kunnath, N.N.: Robustness evaluation of RC frame buildings to progressive collapse, Engineering Structures, 86 (2015), pp. 242–249

[37] Ioani, A., Cucu, H.L.: Vulnerability to Progressive Collapse of Seismically Designed RC Framed Structures Corner Column Case, Buletinul Institutului Politehnic Din Iași, Publicat de Universitatea Tehnică „Gheorghe Asachi din Iași Tomul LVI (LX), Fasc. 4, 2010 Secția Construcții. Ărhitectură, accesed: December 2018.

[38] Li, Y., Lu, X., Guan, H., Ye, L.: Progressive Collapse Resistance Demand of Reinforced Concrete Frames under Catenary Mechanism, ACI Structural Journal, 111 (2014) 5, pp. 1225-1234

[39] Nica, G.B., Pavel, F.: Numerical analysis on the collapse of a RC frame, Mathematical Modelling in Civil Engineering, 12 (2016) 4, pp. 22 - 35, Https://doi.org/10.1515/mmce-2016-0015

[40] Rakshith, K.G., Radhakrishna: Progressive collapse analysis of reinforced concrete framed structure, Internat. Journal of Research in Engineering and Technology, IC-RICE Conference Issue (2013), pp. 36-40

[41] Tsai, M.H.: Evaluation of different loading simulation approaches for progressive collapse analysis of regular building frames, Stucture and Infrastr. Engineering, 8 (2012) 8, , pp. 765-779

[42] Weng, J., Lee, C.K, Kang, K.H. Lim, N.S.: Damage assessment for reinforced concrete frames subject to progressive collapse, Engineering Structures, 149 (2017), pp. 147–160

[43] Shayanfar, M.A., Javidan, M.M.: Progressive Collapse-Resisting Mechanisms and Robustness of RC Frame–Shear Wall Structures, Journal of Performance of Constr. Facilities, 31 (2017) 5, Https://doi.org/10.1061/(ASCE)CF.1943-5509.0001012

[44] Palmisano, F.: Mitigation of progressive collapse by the actiavation of the elesto-plastic catenary behaviour of RC slab structures, The Open Construction ABD Building Techn. J., 8 (2014), pp. 122-131

[45] Starossek, U.: Topology of progressive collapse, Engineering Structures, 29 (2007) 9, pp. 2302-2307

[46] Sasany, M., Kropelnicki, J.: Progressive Collapse analysis of an RC structure, The Struct. Design of Tall and Special BuidingS, 17 (2008), pp. 757-771

[47] Elshaer, A., Mostafa, H., Salem, H.: Progressive collapse assessment of multidtory RC structures subjected to seismic actions, KSCE J. of Civil Engineeering, 21 (2017), pp. 184-194

[48] Tsai, M.H., Lin, B.H.: Investigation of progressive collapse resitance and inelastic response for an earthquake-resistant RC buildin subjected to column failure, Enginering Structures, 30 (2008) 12, pp. 3619-3628

[49] Villaverde, R.: Methods to Assess the Seismic Collapse Capacity of Building Structures: State of the Art, JOURNAL OF STRUCTURAL ENGINEERING, 133 (2007) 1, Https://doi.org/https://doi.org/10.1061/(ASCE)0733-9445(2007)133:1(57)

[50] Stephen, D., Lam, D., Forth, J., Tsavdaridis, K.: An Evaluation of Modelling Approaches and Column Removal Time on Progressive Collapse of Building. Journal of Constructional Steel Research, 153 (2018), pp. 243-253

[51] Rohani, M., Naji, A.: Progressive collapse analysis of RC structures: A simplified procedure, European J. of Eng. Research and Science, 2 (2017) 10, pp. 7-12

[52] Ellingwood, B.R., Smilowitz, R., Dusenberry, D.O., Duthin, D., Carino, N.J.: Best practice for reducing the Potential for Progressive Collapse in Buildings, NISTIR 7396, 2007

[53] Ellingwood, B.R.: Load and Resistance Factor Criteria for Progressive Collapse Design, 2002, https://cdn.ymaws.com/www.nibs.org/resource/resmgr/mmc/wppc_ellingwood_paper.pdf,

[54] Canisius, T.D.G., Sørensen, J.D., Baker, J.W.: Robustness of structural system – a new focus for the Joint Committee on Structural Safety (JCSS), Applic. of Statistics and Probability in Civil Eng.– Kanda, Tkeda, Furuta (eds) (2007), Taylor and Francis Group, London, UK, pp. 1-10

[55] Kokot, S., Solomos, G.: Progressive collapse risk analysis: literature survey, relevant construction standards and guidelines, relevant construction standards and guidelines, European Laboratory for Structural Assessment, Publications Office of the European Union, 2012, pp. 55-59,

[56] Parisi, F., Adam, J.M., Sagaseta, J., Lu, X.: Review of experimental research on progressive collapse of RC structures, IF CRASC'17, Politechnico di Milano, 14-16 Septembre 2017, pp. 265-376

[57] Fu, F.: Progressive collapse design and analysis of multistorey buildings from Structural analysis and design to prevent disproportionate collapse CRC press, https://ww.routledgehandbooks.com/doi/10.1201/b19662-3 , Accessed: 06 Jan 2019

[58] Lu, D.-G., Song, P., Cui, S., Chen, Z.: Vertical Incremental Dynamic Analysis for Assessing Progressive Collapse Resistance and Failure Modes of Structures, 4th International Workshop on Reliable Engineering Computing (REC 2010), NU of Singapore, 2010

[59] Nethercot, D.A.: Design of Building Structures to improve their Resistance to Progressive Collapse, PROCIDIA ENGINEERING, 14 (2011), pp. 1-13

[60] Ćosić, M., Folić, R.: Performance Analysis of Damaged Buildings Applying Scenario of Related Non-Linear Analyses and Damage Coefficient, Building Materials and Structures, 58 (2015) 3, pp. 3-27

[61] Parisi, F., Scalvenzi, M., Brunesi, E.: Performance limit states for progressive collapse analysis of reinforced concrete framed buildings, Structural Concrete, 20 (2019) 1; pp. 68–84, Https://doi.org/10.1002/suco.201800039

[62] CEN, EN1998- Part 3: Assessment and retrofitting of buildings, 2005

[63] FEMA 356. Prestandard and Commentary for the Seismic Rehabilitation of Buildings, Prepared by ASCE, Prepared for FEMA, November 2000.

[64] Smith, M.: Progressive Collapse Assessment-Non-linear behaviour of concrete structures in damaged state, Master's thesis, TU, Delft, 2007

[65] Attia, F., Salem, H., Yehia, N.: Progressive Collapse Assessment of Mid-Rise Reinforced Concrete Flat Slab Structures, Structural Concrete, 18 (2017) 3, pp. 409-420, Https://doi.org/10.1002/suco.201600051

[66] Bao, Y., Kunnath, S.K.: Simplified progressive collapse simulation of RC frame-wall structures, Engineering Structures, 32 (2010) 10, pp. 3153-3162.

[67] Lu, X., Lin, X., Ma, Y., Li, Y., Ye, L.: Numerical simulation for the progressive collapse of concrete building due to earthquake, 14th Word Conference on Earthquake Engineering, Beijing, China, October 12/17, 2008

[68] CSi Knowledge Base, Etabs, Modeling Concrete Cracked Section Properties for Building Analysis, Added by Truly Guzman, last edited by Truly Guzman on Jun 15, 2017, accesed: August 2020

[69] CSi Knowledge Base, Etabs, Panel Zone and Rigid Offset, Added by Truly Guzman, last edited by Mohamad Ali-Ahmad on Sep 12, 2014, accesed: August 2020

[70] CSi Knowledge Base, Technical Knowledge Base, Ritz vs. Eigen Vectors, Added by Riaz, last edited by Jessica Napier on Apr 04, 2014, accessed: August 2020

[71] ETABS, Computers and Structures, Inc., 2016

[72] Kwasniewski, L.: Nonlinear dynamic simulations of progressive collapse for a multistory building, Engineering Structures, 32 (2010) 5, pp. 1223-1235

[73] Marjanishvili, S.M.: Progressive analysis procedures for progressive collapse, Journal of Performance Constructed Facilities, ASCE, 18 (2004) 2, pp. 79-85

[74] Lu, D.G., Cui,S.S., Song, P.Y., Chen, Z.H.: Robustness assessment for progressive collapse of framed structures using Pushdown analysis method, 4th Inter. Workshop on Reliable Engineering Computing (REC 2010), NU of Singapore, 2010, Https://doi.org/10.3850/978-981-08-5118.7-063

[75] Singhania, A., Khatuja, V., Singh Thakur, V., Rao, C.B.K.: Simplified Analysis of RC Framed Structures for Progressive Collapse, Int. Journal of Scientific & Research, 4 (2013) 5, pp. 264- 271

[76] Izzudin, B.A., Vlassis, A.G. Elghaozuli, A.Y. Nethart, D.A.: Progressive collapse of multi-story buildings due to sudden column loss - Part I: Simplified assessment framwork, Engineering Structures, 30 (2008) 5, pp. 1308-1318

[77] Brunesi, E., Nascimbene, R., Parisi, F.: Progressive collapse fragility models of RC framed buildings based on pushdown analysis, ECCOMAS Congress 2016, VII Eur. Congress on Comput. Methods in Applied Sciences and Engineering; M. Papadrakakis, et al. (eds.), Crete Island, Greece, 5–10 June 2016. Https://doi.org/10.7712/100016.2155.5285.

[78] Brunesi, E., Nascimbene, R., Parisi, F., Augenti, N.: Progressive collapse fragility of reinforced concrete framed structures through incremental dynamic analysis, Engineering Structures, 104 (2015), pp. 65-79

[79] Agnew, E., Marjanishvili, S.: Dynamic analysis procedures for progressive collapse. STRUCTURE MAGAZINE (2006), pp. 24–27

[80] Bao, Y., Main, J.A., Noh, S.-Y.: Evaluation of Structural Robustness against Column Loss: Methodology and Application to RC frame Buidings, ASCE Journal of Structural Engineering, 143 (2017) 8, pp. 12.

[81] Kumari, D.: Effect of span length in progressive collapse of multi-storey RC building under corner and middle column removal scenario, Int. Journal of Civil Eng. and Technology, 9 (2018) 3, pp. 449-466

[82] Kevins, P., Tushar, P.: Effects of Irregularity on Progressive Collapse of RCC Building, Imperial Journal of Interdisciplinary Research (IJIR), 3 (2017) 4, pp. 1637-1647

[83] CEN, EN 1992: Design of concrete structures, Part 1-1: General rules and rules for buildings, Brussels, 2004

[84] CEN, EN1998-1: Design of structures for earthquake resistance - General rules, seismic actions, rules for buildings, 2004

[85] Mander, J., Priestley, M., Park, R.: Theoretical Stress-Strain Model for Confined Concrete, Journal of Structural Engineering, 114 (1988) 8, pp. 1804-1825

[86] Ćosić, M., Folić, R., Brčić, S.: An Overview of Modern Seismic Analyses with Different Ways of Damping Introduction, Building Materials and Structures, 60 (2017) 1, pp. 3-30

[87] Adom-Asamoah, M., Ankamah, N.O.: Effect of design ductility on the progressive collapse potentional of RC frame structures designed to EC 8, American Journal of Civil Engineering, 4 (2016) 2, pp. 24-33

[88] Wong, J.M., Sommer. A., Briggs, K., Cenk, E.: Effective stiffness for modeling reinforced concrete structures: a literature review. Structure Magazine, 24 (2017), pp. 18-21

[89] ACI 318-11: Building Code Requirements for Structural Concrete and Commentary, American Concrete Institute, August 2011

[90] CSi Knowledge Base, Etabs, Modeling concrete cracked section properties for building analysis, Created by Truly Guzman, last modified on Jun 15, 2017, accesed: August 2020

[91] Paulay, T., Priestley, M.J.N.: Seismic Design of Reinforced Concrete and Masonry Buildings, John Wiley and Sons, New York, U.S.A., (1992), pp. 767

[92] CSi Knowledge Base, Etabs, Caltrans vs. fiber hinge, last modified by Jessica Napier on Jun 10, 2014, accesed: August 2020

[93] EasyFit, MathWave Technologies

[94] Baker, J.W.: Efficient analytical fragility function fitting using dynamic structural analysis, EARTHQUAKE SPECTRA, 31 (2015) 1, pp. 579-599